

Research Article



Glycolytic and oxidative muscles under acute glucose supplementation differ in their metabolic responses to fatty acyl-CoA synthetase gene suppression

Yun Hee Jung  and So Young Bu 

Department of Food and Nutrition, Daegu University, Gyeongsan 38453, Korea



Received: Dec 24, 2021
Revised: Jan 20, 2022
Accepted: Jan 26, 2022
Published online: Feb 15, 2022


Correspondence to

So Young Bu

Department of Food and Nutrition, College of Engineering, Daegu University, 201 Daegudae-ro, Gyeongsan 38453, Korea.
Tel: +82-53-850-6832
Email: busy@daegu.ac.kr

© 2022 The Korean Nutrition Society
This is an Open Access article distributed under the terms of the Creative Commons Attribution Non-Commercial License (<http://creativecommons.org/licenses/by-nc/3.0/>) which permits unrestricted non-commercial use, distribution, and reproduction in any medium, provided the original work is properly cited.

ORCID iDs

Yun Hee Jung 
<https://orcid.org/0000-0002-5817-3401>
So Young Bu 
<https://orcid.org/0000-0001-9801-5435>

Funding

This work was supported by the National Research Foundation of Korea (NRF) grant funded by the Korea government (MSIT) (No. 2021R1F1A1062898).

Conflict of Interest

There are no financial or other issues that might lead to conflict of interest.

<https://e-jnh.org>

ABSTRACT

Purpose: Skeletal muscles display significant heterogeneity in metabolic responses, owing to the composition of metabolically distinct fiber types. Recently, numerous studies have reported that in skeletal muscles, suppression of genes related to fatty acid channeling alters the triacylglycerol (TAG) synthesis and switches the energy substrates. However, such responses may differ, depending on the type of muscle fiber. Hence, we conducted in vitro and animal studies to compare the metabolic responses of different types of skeletal muscle fibers to the deficiency of fatty acyl-CoA synthetase (*Acs16*), one of the main fatty acid-activating enzymes.

Methods: Differentiated skeletal myotubes were transfected with selected *Acs16* short interfering RNA (siRNA), and C57BL/6J mice were subjected to siRNA to induce *Acs16* deficiency. TAG accumulation and expression levels of insulin signaling proteins in response to acute glucose supplementation were measured in immortalized cell-based skeletal myotubes, oxidative muscles (OM), and glycolytic muscles (GM) derived from the animals.

Results: Under conditions of high glucose supplementation, suppression of the *Acs16* gene resulted in decreased TAG and glycogen synthesis in the C2C12 skeletal myotubes. The expression of *Glut4*, a glucose transporter, was similarly downregulated. In the animal study, the level of TAG accumulation in OM was higher than levels determined in GM. However, a similar decrease in TAG accumulation was obtained in the two muscle types in response to *Acs16* suppression. Moreover, *Acs16* suppression enhanced the phosphorylation of insulin signaling proteins (Foxo-1, mTORc-1) only in GM, while no such changes were observed in OM. In addition, the induction ratio of phosphorylated proteins in response to glucose or *Acs16* suppression was significantly higher in GM than in OM.

Conclusion: The results of this study demonstrate that *Acs16* differentially regulates the energy metabolism of skeletal muscles in response to glucose supplementation, thereby indicating that the fiber type or fiber composition of mixed muscles may skew the results of metabolic studies.

Keywords: skeletal muscle; muscle fibers; glucose

INTRODUCTION

The skeletal muscle contributes substantially to whole-body glucose uptake and oxidation of energy substrates, including glucose and fatty acids. Hence, defects in the metabolic capacity of skeletal muscles are associated with insulin resistance or diabetes, as reported in adipose tissue and the liver [1,2]. For instance, increased fatty acid conversion to acyl-CoAs and its esterification to triacylglycerol (TAG) in skeletal muscle significantly correlate with whole-body insulin action in animal models and human subjects [3,4]. Moreover, high concentrations of intracellular fatty acids and ketone bodies weaken insulin action in the rat diaphragm muscles [5].

Skeletal muscle has specialized cellular characteristics depending on the type of muscle fiber: oxidative and glycolytic fibers. The proportion of these fiber types varies by muscle group and can be switched based on physiological conditions [6-8]. Oxidative fibers are mainly involved in the postural integration of muscles and long-term energy supply. With high mitochondrial content, they rely heavily on oxidative phosphorylation. These muscles are slowly contracted and are resistance to fatigue. Glycolytic fibers have a lower mitochondrial content and less reliance on oxidative phosphorylation. These muscles contract slowly and are resistant to fatigue. Glycolytic fibers have lower mitochondrial content and are less reliant on oxidative phosphorylation. These muscles contract rapidly but have low fatigue resistance and are involved in muscle groups used for steering movement [9,10]. Owing to their distinctive metabolic characteristics and location within the whole muscle tissue, their responses to various metabolic challenges may differ. Compared to glycolytic fibers, oxidative muscle (OM) fibers have a greater capability to utilize and store cellular lipids because of their higher mitochondrial content and respiratory enzyme activity [9]. For example, a high-fat diet increased TAG accumulation in the soleus muscle, which is mainly composed of OM fibers [11], and the increase in skeletal muscle TAG content with endurance exercise occurs primarily in OMs [12]. In addition, OMs sensitively control β -oxidation and are prone to muscle weakness [13]. In contrast, glycolytic fibers mostly rely on carbohydrates as an energy source and have a lower capacity for lipid oxidation; therefore, they do not store as many lipids as oxidative fibers [6,14]. A higher proportion of glycolytic fibers is positively correlated with insulin resistance in human subjects [6], and the levels of protein kinase-C, enzymes that interfere with insulin signaling are highly responsive to fructose in Sprague-Dawley rats [10]. The metabolic changes induced by TAG-modifying enzymes were distinct according to fiber type. Skeletal muscle-specific *Dgat2*-overexpressing mice had increased the content of TAG, unsaturated fatty acyl-CoAs, and lipid-derived inflammatory mediators in the glycolytic muscle (GM), which were associated with defects in insulin signaling and insulin-stimulated glucose uptake in this tissue [15]. This suggests that defects in fatty acid flux and TAG synthesis in skeletal muscle may have different consequences on insulin resistance depending on the fiber type of the skeletal muscle.

We recently reported that intramyocellular *Acs16* deficiency alters glucose and lipid metabolism in C2C12 cells [16] and skeletal muscle tissue in an animal model [17]. Long-chain acyl-CoA synthetase (ACSL) activates fatty acids to acyl-CoA and mediates the initial step in lipid metabolism, including TAG synthesis and fatty acid oxidation. *Acs1* has been suggested to guide cellular fatty acids toward different metabolic fates and influence lipid-mediated signaling [18,19]. Our previous study showed that the suppression of *Acs16*, an *Acs1* isoform expressed in the skeletal muscle, increased the loss of free fatty acids from their acylation into TAG and decreased 2-deoxyglucose uptake in differentiated skeletal myotubes, indicating that *Acs16* contributes to the glucose-fatty acid cycle by channeling intracellular

fatty acid turnover [16]. In *Acsf6*-reduced animals, decreased TAG accumulation in skeletal muscle enhanced glucose tolerance without significant changes in insulin signaling proteins, insulin receptor substrate (IRS)-1, and AKT [17]. Our two recent reports on animal and cell culture studies [16,17] have shown little difference in the changes in signaling molecules in the insulin cascade. Compared to control cells, *Acsf6* suppression in C2C12 cell cultures causes defects in Akt phosphorylation in differentiated skeletal myotubes upon insulin treatment [16]. However, in animal studies, *Acsf6* reduction did not significantly alter the phosphorylation of IRS-1 or Akt in skeletal muscle tissues in response to acute glucose supplementation [17]. Such a discrepancy in the contribution of decreased TAG to insulin signaling between cell cultures and muscle tissues of animals may lead to inconclusive results regarding the role of *Acsf6* in insulin resistance. However, our previous animal study utilized whole muscle tissues, and insulin signaling in different muscle fiber types has not been addressed. Differentiated myotubes derived from C2C12 cells are metabolically stable without physiological stress; hence, it is difficult to judge the fiber types of these myotubes compared with skeletal muscle fibers in live animals. Owing to significant heterogeneity, it is possible that metabolic responses in skeletal muscle tissue may either be under- or overestimated, or discrepancies may occur based on the composition of muscle fibers. Hence, we compared the metabolic responses of different types of skeletal muscle fibers to *Acsf6* deficiency under acute high glucose supplementation in cell cultures and animal studies.

METHODS

C2C12 cell culture

Mouse C2C12 myoblasts were obtained from the American Type Culture Collection (ATCC, Manassas, VA, USA) and cultured in Dulbecco's modified Eagle's medium (DMEM) supplemented with 23 mM HEPES, 26 mM sodium bicarbonate, 50 IU/mL penicillin, 50 µg/mL streptomycin, 5.5 mM glucose, and 10% fetal bovine serum at 37°C in a humidified incubator with 5% CO₂. Once the cells reached 90–100% confluence (day 0), the cell culture medium was replaced with DMEM supplemented with 2% horse serum and 5.5 mM glucose for differentiation into skeletal myotubes.

RNA interference

Initially, four sets of *Acsf6* siRNA duplexes (GenBank accession number NM_14482; Qiagen, Germantown, MD, USA) were commercially synthesized (Qiagen) [17]. One siRNA sequence targeting mouse *Acsf6* (Gene Bank, TM accession number NM_144823) covering the nucleotide positions of 1389–1409, which was used in a previous animal study [17], was utilized. The siRNA knockdown efficiency was validated in cell cultures under acute glucose supplementation, and a non-specific sequence-targeting siRNA served as a control siRNA. The interference RNA was transfected into the differentiated skeletal myotubes at 250 ng of siRNA per 2.5×10^5 cells using transfection reagent (Qiagen) three days after the cells were differentiated. After 6 hours, the medium was replaced with DMEM supplemented with 2% horse serum, 10 nM insulin, 10 nM dexamethasone, 5.5 mM glucose, and antibiotics. At 44 hours after siRNA transfection, cells were fasted in media containing no glucose for 5.5 hours, treated with 25 mM glucose for 30 minutes, and then harvested.

Cell viability

Cell viability was assessed using the 3-(4,5-dimethylthiazol-2-yl)-2,5-diphenyltetrazolium bromide (MTT) assay in a commercial protocol (Ez-Cytox; DoGen Bio, Seoul, Korea). The

cells were transfected with siRNA, treated with high glucose, incubated with an MTT reagent, and the colored formazan products were measured at 450 nm using a Sunrise ELISA plate reader (Tecan, Germany).

Quantitative real-time polymerase chain reaction (PCR)

At the indicated time points, cells were harvested using TRIzol reagent (Invitrogen, Waltham, MA, USA), and total cellular RNA was isolated. First-strand cDNA was synthesized using SuperScript III reverse transcriptase and random hexamer primers (Takara Bio, San Jose, CA, USA). After incubation with RNase H, the cDNA was mixed with 2X SYBR Green PCR Master Mix (Takara Bio) and probed for the target genes by real-time PCR quantification on a Takara PCR system (Takara Bio Inc., Shiga, Japan). Fluorescence emission data were acquired for 45 cycles at an annealing temperature of 60°C. Primers used for each gene are listed in **Table 1**. Data were analyzed using the $\Delta\Delta C_t$ method, and the mRNA abundance of each gene was normalized to *Rpl32*.

Acs16 deficient animal model

The animal protocols were approved by the Institutional Animal Care and Use Committee of Daegu University (DAEGU-2014-12-0904-001). Eight-week-old C57BL/6J male mice were maintained under controlled temperature (20–22°C) and lighting (12:12 h light-dark cycle). The transient *Acs16* deficient animal model was developed [17]. Consistent with the cell culture study, non-specific sequence-targeting siRNA (Qiagen) was used as a control siRNA. Mice administered either control siRNA or *Acs16* siRNA were fed an AIN-93 diet (D10012G, Research Diet, New Brunswick, NJ, USA) and had free access to water for 14 days. The percentages of total calories in protein, carbohydrate, and fat in the AIN-93 diet were 20%, 64%, and 16%, respectively, and soybean oil (70 g/kg) was the fat source of this diet. At the end of the experiment, the animals were fasted overnight and injected intraperitoneally with 20% dextrose or saline (vehicle) 30 minutes prior to euthanization. Skeletal muscle tissues of one leg were separated by either the white head of gastrocnemius to obtain the GM or the red fiber area of the soleus muscle for the OM, and snap-frozen until further analysis.

Measurement of total TAG accumulation

At 44 hours after siRNA transfection, the differentiated C2C12 skeletal myotubes were fasted and incubated with 25 mM glucose for 30 minutes. The cells were washed twice with 1% BSA in PBS at 37°C, and the cellular lipids were extracted [20]. Extracted lipids were dried under nitrogen vapor, and total TAGs were measured. To measure the total TAG content in animal tissues, tissues were homogenized in PBS, and lipids were extracted [20]. The total TAG content in cell cultures and animal tissues was measured using a commercial kit (Stanbio Laboratory, Elkhart, IN, USA).

Table 1. Primer sequences for quantitative polymerase chain reaction

Gene	Forward primer (5'-3')	Reverse primer (5'-3')
<i>Acs11</i>	ACCATGTACGATGGCTTCCA	TCATAGGGCTGGTTGGCTT
<i>Acs16</i>	ACGAGGACAGGACAAAGGAG	CTCTGG CGCAACATATTCCC
<i>Glut4</i>	TTGGGAAGGAAAAGGGCTAT	GAGGAACCGTCCAAGAATGA
<i>Gck</i>	TATGAAGACCGCCAATGT	CCGCCAATGATCTTTTC
<i>Gpat1</i>	CAACACCATCCCCGACATC	CCGCAGCATTCTGATAACGC
<i>Rpl32</i>	AACCCAGAGGCATTGACAAC	ATTGTGGACCAGGAACCTTGC

Western blotting

To measure protein expression, cell or animal tissue homogenates were lysed in a 0.1% Triton X-100 solution composed of 10 mM Tris-HCl (pH 7.4), 150 mM NaCl, 1% phosphatase inhibitor, and 1% protease inhibitor cocktail (Roche Life Science, Indianapolis, IN, USA). Aliquots of total proteins (10–20 µg) were mixed with sample loading buffer containing 50 mM Tris (pH 6.8), 2% SDS, 10% glycerol, 1% bromophenol blue, and 15% β-mercaptoethanol, and denatured at 100°C for 10 min. Proteins were separated by SDS-polyacrylamide gel electrophoresis and transferred to polyvinylidene difluoride membranes (Millipore Sigma, Burlington, MA, USA). Proteins electrotransferred onto the membrane were verified by Ponceau S staining. The membrane was then blocked with 1% fish-gelatin in Tris-buffered saline (TBS, pH 7.4) with 0.05% Tween 20. The membranes were probed with GLUT4 (Santa Cruz Biotechnology, TX, USA), β-actin (Sigma), class O forkhead box transcription factor (FoxO)-1, p-FoxO-1, ribosomal protein S6 kinase (p70S6K), p-p70S6K, mammalian target of rapamycin complex (mTORc)-1, and p-mTORc-1 (Cell Signaling Technology, Danvers, MA, USA) antibodies. Following incubation with a horseradish peroxidase-conjugated secondary antibody according to the origin species of epitope in the primary antibody, antigen-reacted protein bands were detected by an ECL chemiluminescent assay. Images were acquired using a Fusion Solo (Vilber Lourmat, Marne-la-Vallée, France) or LAS 4000 (GE Healthcare, Dresher, PA, USA). The density of protein bands on individual blots was measured using ImageJ software (National Institutes of Health, Bethesda, MD, USA).

Statistical analysis

Each experiment was performed more than twice, and the data are expressed as mean ± SEM. All comparisons of control versus *Acs16* deficiency in both cell culture and animal studies were performed using Student's t-test. The significance level was set at $p < 0.05$.

RESULTS

Efficiency validation of *Acs16* siRNA under acute glucose supplementation

The knockdown efficiency of *Acs16* siRNA was tested in differentiated C2C12 skeletal myotubes supplemented with high (25 mM) glucose. Quantitative reverse transcription-PCR revealed that the selected siRNA sequence substantially reduced the level of *Acs16* mRNA by more than 70% under high glucose conditions (**Fig. 1A**), which was similar to the previously reported knockdown efficiency of *Acs16* siRNA under no or basal (5 mM) glucose conditions [16]. Moreover, we confirmed that cell viability was over 90% 50 hours after siRNA transfection (**Fig. 1B**). There was no high glucose-induced compensation in the expression of the following genes involved in initial fatty acid channeling: *Acs11*, a highly expressed *Acs1* gene in skeletal muscle [3], and *Gpat1*, which is involved in fatty acid acylation of the glycerol backbone [21] (**Fig. 1C**).

Lipid accumulation and genes involved in glucose utilization in skeletal myotubes following *Acs16* knockdown

Given the roles of *Acs16* isoforms in lipid accumulation and *de novo* lipogenesis, which were reported in a previous study [16], we explored the effect of *Acs16* knockdown on cellular TAG accumulation in response to acute glucose treatment. The total TAG content was significantly decreased by 30% in cells transfected with *Acs16* siRNA in high glucose-supplemented media (**Fig. 2A**). However, knockdown of *Acs16* suppressed *Glut4* mRNA expression in basal media

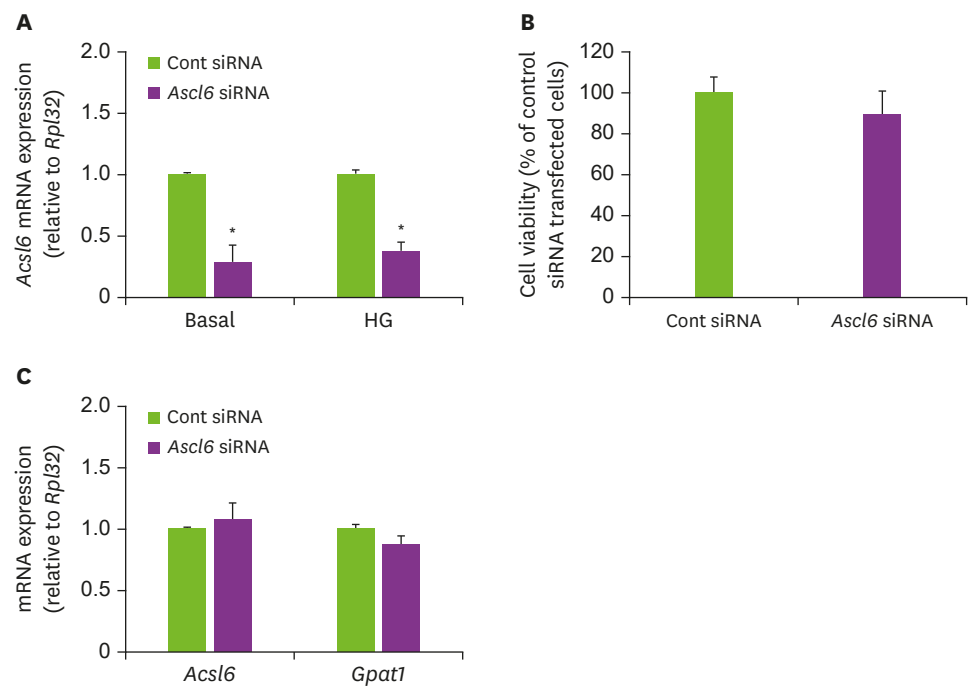


Fig. 1. Validation of the effect of *Acs16* siRNA under high glucose condition in differentiated myotubes. C2C12 cells were differentiated into skeletal myotubes and transfected with control or *Acs16* siRNA duplexes. After 44 hours, the cells were fasted for 5.5 hours and treated with 25 mM glucose for 30 minutes, and total RNA was extracted. (A) The mRNA abundance of *Acs16* was quantified using quantitative reverse transcription polymerase chain reaction and normalized to that of *Rpl-32*. (B) The cell viability was assessed. (C) The abundances of *Acs16* and *Gpat1* were measured. The data are expressed as arbitrary values relative to the control siRNA-transfected cells. siRNA, short interfering RNA. $p < 0.05$, compared with controls.

and did not change *Glut4* expression in high glucose-treated media (Fig. 2B). The level of *Gck* mRNA was not altered by *Acs16* knockdown (Fig. 2C).

Comparison of TAG accumulation and gene expression of glucose utilization in skeletal muscle of *Acs16* deficient mice

In this study, we measured TAG accumulation in the GM and OM, two metabolically different types of skeletal muscle [10]. The atelocollagen mixture of *Acs16* siRNA instillation decreased TAG content by approximately 50% in both the GM and OM in mice fed the AIN-93 diet (Table 2). When we converted this value to the percentage of TAG in total hind limb muscles,

Table 2. TAG accumulation and partitioning in different types of skeletal muscle

Outcomes	Control	<i>Acs16</i> deficient	p-value
Conc. of TAG accumulation (mg/g protein)			
Total hind limb muscle	21.3 ± 4.6 ³⁾	10.1 ± 1.6	0.0163 ²⁾
Soleus (type I slow twitch)	18.6 ± 4.5	9.1 ± 1.7	0.0356
Gastrocnemius (type I fast twitch)	2.3 ± 0.8 ³⁾	1.0 ± 0.3 ³⁾	-
TAG distribution (% of total muscle lipids)			
Soleus	87.6 ± 21.4	90.6 ± 16.7	0.3481
Gastrocnemius	10.7 ± 3.5	9.6 ± 3.3	0.3934
Ratio of TAG partitioning			
Soleus/Gastrocnemius	8.2	9.5	N.A.

¹⁾Data are expressed as mean ± SEM. ²⁾Student's t-test was performed to assess the difference between control and *Acs16* deficient animals. ³⁾Values for TAG in gastrocnemius muscles were previously reported as a part of graphic image [17].

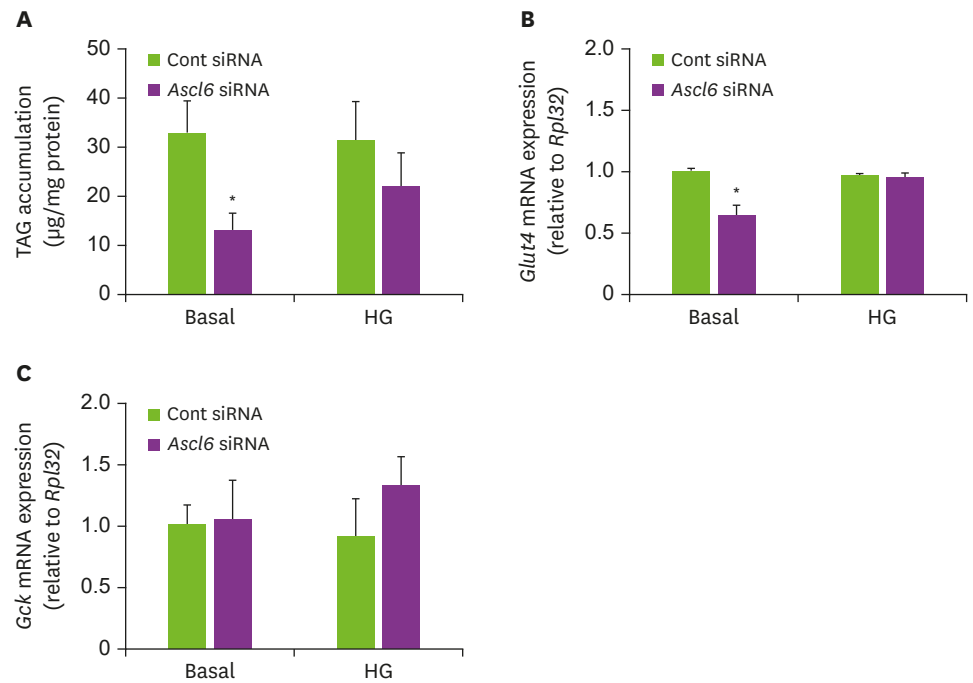


Fig. 2. *Acs16* siRNA mediated changes in TAG accumulation and genes of glucose utilization in differentiated skeletal myotubes under acute glucose supplementation.

Differentiated skeletal myotubes were transfected with the *Acs16* siRNA. After 44 hours, the cells were fasted for 5.5 hours and treated with 25 mM glucose for 30 minutes, and lipids were extracted. (A) The total TAG content was quantified as described in the “Methods” section. The mRNA expression levels of (B) *Glut4* and (C) *Gck* were measured. Data are expressed as the mean \pm SEM from two or three experiments performed in triplicate. TAG, triacylglycerol; siRNA, short interfering RNA. $p < 0.05$, compared with control siRNAs.

the TAG percentages in GM and OM were $9.6\% \pm 3.3\%$ and $90.6\% \pm 16.7\%$, respectively. However, these values were not significantly different between *Acs16* knockdown and control animals. In total hind limb muscle, *Glut4* mRNA expression was not altered in *Acs16* deficient animals (Fig. 3A). Hence, we further measured the level of *Glut4* protein expression in the GM and OM (Fig. 3B and C). The basal expression level of *Glut4* protein was higher in OM than in GM. Protein expression of *Glut4* tended to be increased only in the GM in *Acs16* deficient animals, but the degree of change was not statistically significant.

Distinguished responses on insulin signaling proteins in GM and OM of *Acs16* deficient animals

In a previous study, *Acs16* suppressed animals exhibited enhanced glucose tolerance without changes in the glucose disposal capacity of skeletal muscle and the phosphorylation of IRS-1 or Akt in skeletal muscle [17]. We speculated that the lack of alteration in insulin signaling may be due to the heterogeneous nature of skeletal muscle fibers. Thus, we investigated the phosphorylation of subsequent levels of insulin signaling proteins in OM and GM. In GM, the phosphorylation of FoxO-1, mTORC-1, and p70S6K significantly increased in response to acute glucose supplementation (Fig. 4A, C, and E), whereas only p70S6K signaling was observed in OM (Fig. 4E). *Acs16* deficiency increased the level of phosphorylation of FoxO-1 and mTORC-1 protein only in the GM (Fig. 4B and D). *Acs16* reduction did not affect p70S6K in either the GM or the OM of the animals (Fig. 4F). The induction ratios of phosphorylated FoxO-1 and mTORC-1 in response to glucose were 2.0% and 3.0%, respectively, in GM (Fig. 5). The fold-change in the phosphorylation of mTORC-1 by *Acs16* suppression was significantly higher in

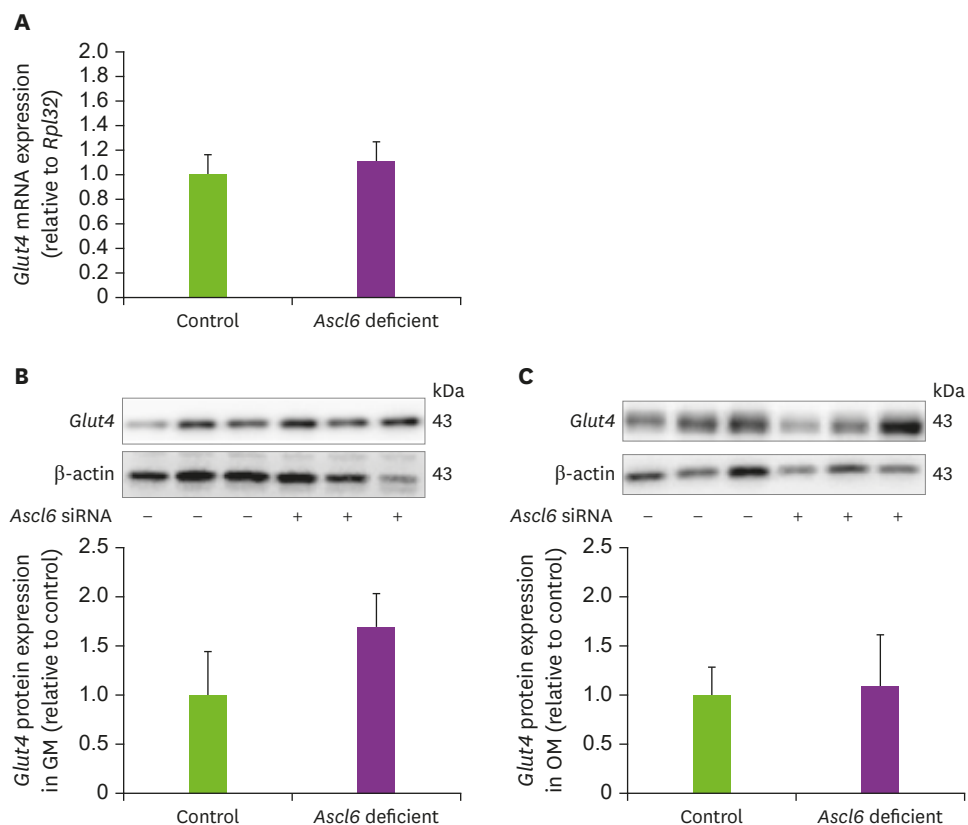


Fig. 3. Expression level of *Glut4* in skeletal muscle tissue of *Acs16* deficient mice.

C57BL/6J mice were administered control siRNA or *Acs16* siRNA ($n = 6/\text{group}$) and fed AIN-93 diet for 10 days. Animals were orally administered a 20% dextrose solution. (A) *Glut4* mRNA was quantified in total hindlimb muscles ($n = 6/\text{group}$). Protein expression of *Glut4* was assessed in the (B) GM and (C) OM. Data are mean \pm SEM. siRNA, short interfering RNA; GM, glycolytic muscle; OM, oxidative muscle. * $p < 0.05$, compared with the control siRNA.

GM than in OM. The fold induction in the phosphorylation of FoxO-1 and p70S6K was not significantly different between OM and GM.

DISCUSSION

Muscle tissue is responsible for a substantial proportion (approximately 80%) of whole-body glucose uptake and utilization; therefore, it plays an important role in the action of insulin and metabolism of energy substrates. Defects in insulin signaling or glucose transport, defined as insulin resistance in skeletal muscle, are an obvious risk factor for type 2 diabetes mellitus. Owing to the heterogeneity of fiber types in skeletal muscle tissue and fundamental differences in their metabolic characteristics [10,14], the results observed from pooled tissues composed of different fiber types could be misrepresented. In this study, we investigated the effect of siRNA-mediated *Acs16* knockdown on lipid accumulation and downstream effectors of insulin signaling, mTORc-1, p70S6K, and FoxO-1 in C2C12-skeletal myotubes, GM, and OM of C57BL/6J mice under glucose supplementation.

Initially, we checked whether high glucose treatment affected siRNA efficiency and compensated for *Acs16* deficiency-induced lipid accumulation. Under high glucose treatment,

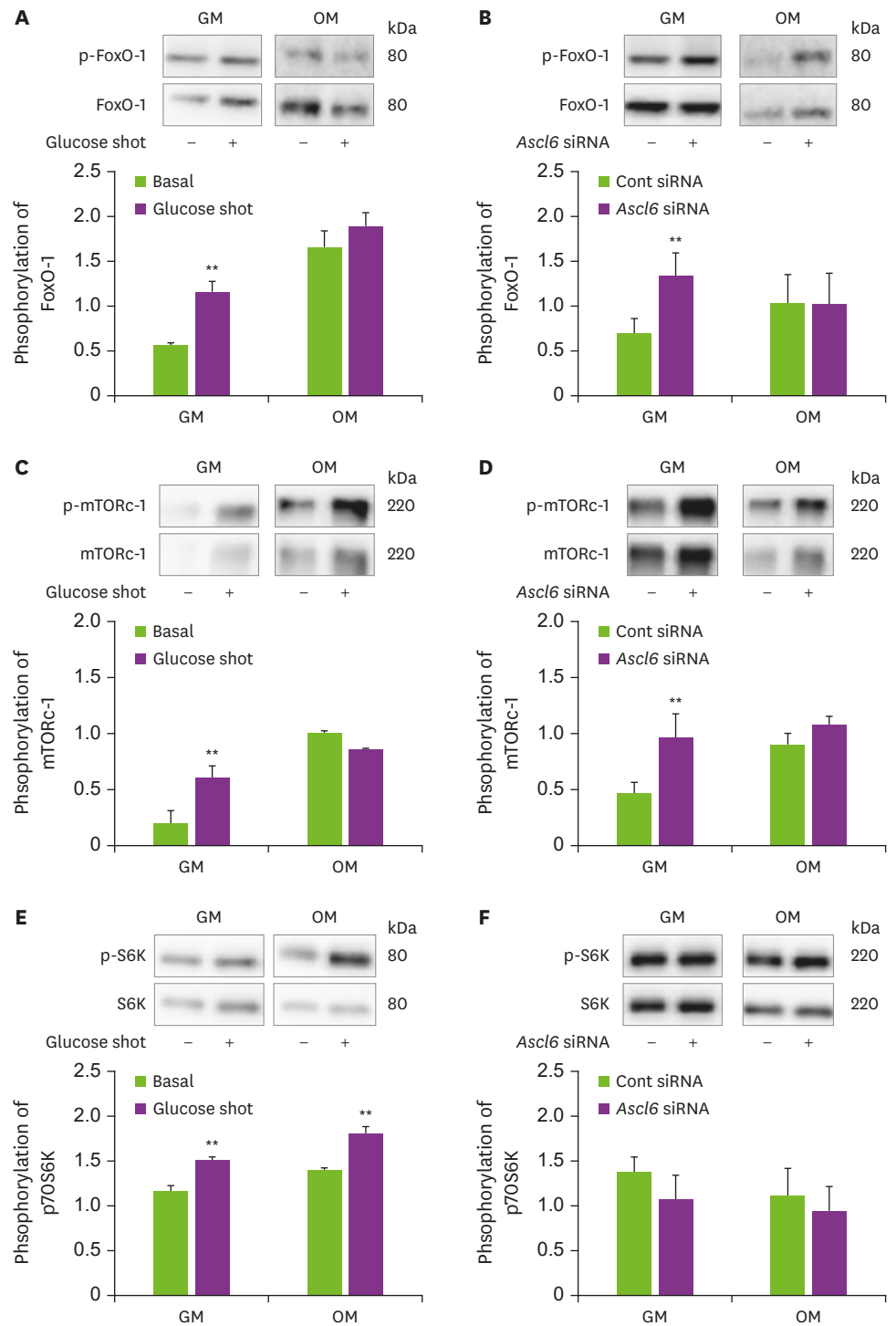


Fig. 4. FoxO-1, mTORC-1, and p70S6K phosphorylation in response to acute glucose supplementation and *Ascl6* knockdown in GM and OM of C57BL/6J mice.

Ascl6 siRNA-administered animals were allowed to fast overnight, followed by oral gavage of 20% dextrose solution. The phosphorylated form of protein in response to glucose shot or *Ascl6* suppression was measured for (A-B) FoxO-1, (C-D) mTORC-1, and (E-F) p70S6K 30 minutes after oral gavage of dextrose (n = 3–4). The density of FoxO-1, mTORC-1, and p70S6K proteins was quantified. Representative bands are presented, and the data are presented as mean ± SEM.

GM, glycolytic muscle; OM, oxidative muscle; siRNA, short interfering RNA.

**p < 0.01, compared to control siRNA.

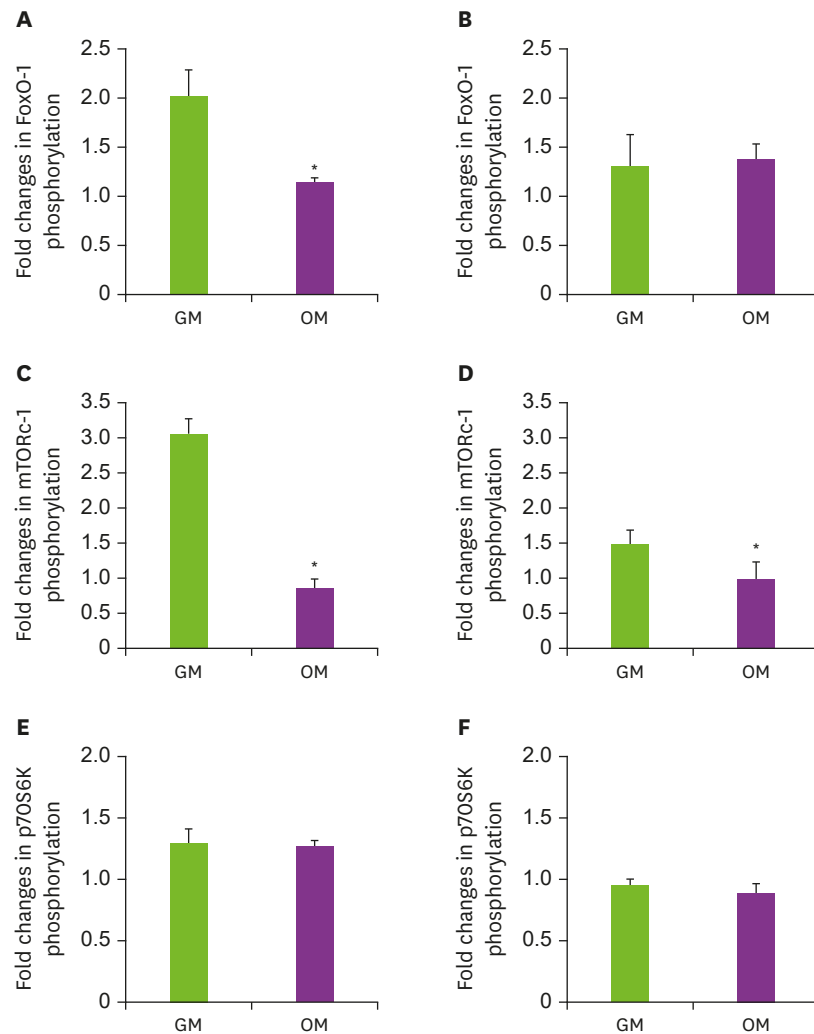


Fig. 5. Comparison of fold changes in FoxO-1, mTORC-1, and p70S6K phosphorylation between GM and OM of *Acs16* deficient C57BL/6 mice.

Phosphorylation of FoxO-1, mTORC-1, and p70S6K was measured and quantified, as shown in Fig. 4. The degree of phosphorylation for each protein was calculated by the relative density of the protein band relative to the non-phosphorylated form. Data are expressed as mean ± SEM.

GM, glycolytic muscle; OM, oxidative muscle.

*p < 0.05, difference between the GM and OM.

the effect of *Acs16* knockdown on lipid accumulation in C2C12 skeletal myotubes was similar to the effects seen in a recent study [16], which showed that *Acs16* siRNA decreased fatty acid uptake and lipid storage in differentiated C2C12 skeletal myotubes, including TAG and phospholipids. In that study, *Acs16* suppression impaired glucose uptake and de novo lipid synthesis from [¹⁴C] acetate [16]. In an animal study, TAG accumulation in OM was significantly higher than in GM in both control and *Acs16* suppressed animals. This observation is in agreement with a previous finding that [¹⁴C] palmitic acid incorporation for TAG deposition and mitochondrial oxidation was greater in the soleus muscle, which has a high content of oxidative fibers [14], and that the oxidative capacity of muscle positively correlated with TAG accumulation in the skeletal muscle of endurance-trained athletes [12]. Hence, these OM properties led to a greater increase in TAG accumulation in the OM. In this study, the *Acs16* deficient mice had decreased TAG content compared to that of control animals, but the percentage of TAG distribution relative to total hindlimb muscle lipids

and the ratio of TAG partitioning in both GM and OM were similar between control and *Acs16* deficient animals. The results indicated that the degree of lipid accumulation differed between the GM and OM, but the acute challenge of high glucose did not compensate for the *Acs16* siRNA mediated decrease in lipid accumulation in both types of muscle fibers.

This study also examined the level of *Glut4*, one of the main glucose transporters, in C2C12 cells, GM, and OM of the study animals. In C2C12 cells, acute glucose supplementation did not induce *Glut4* or *Gck* mRNA expression in either control or *Acs16* siRNA-transfected cells, indicating that acute glucose did not interfere with *Acs16* siRNA-induced changes in skeletal myotubes. The results from animal tissues revealed a tendency of higher GLUT4 protein expression in the GM in *Acs16* deficient animals, although *Acs16* deficiency did not significantly alter GLUT4 protein expression in either type of muscle fiber. Insulin- or hyperglycemia-induced glucose uptake in skeletal muscle has mostly been assessed through the degree of GLUT4 translocation rather than the level of mRNA or protein expression. A previous study [22] reported that stimulation of C2C12 cells with 25 mmol/L glucose for 10 minutes induced a comparable increase in GLUT4 protein levels in the plasma membrane, and acute hyperglycemia induced an increase in GLUT4 content in the plasma membrane by more than two-fold in Wistar rats [22]. Since *Glut4* was analyzed in whole tissue homogenate, the expression differences in membrane and cytosolic fractions due to translocation could not be determined in this study. Nevertheless, many studies have suggested substantial differences in glucose uptake and utilization between glycolytic and oxidative fibers [23-25]. Because glycolytic fibers have a tendency for basal glucose uptake with a higher rate, fewer insulin receptors, and less *Glut4* content than oxidative fibers [24,25], GM might not need to necessarily respond to acute glucose supplementation in this study. In addition, Galante et al. [22] showed that the translocation of *Glut4* beyond its mRNA or protein expression occurs in a much shorter time frame than in this study. In this study, *Glut4* mRNA in cell cultures and *Glut4* protein expression were measured 30 minutes after glucose supplementation, and the time point of tissue harvesting upon glucose supplementation in fasted animals, in some ways, was not appropriate to induce a detectable change in *Glut4* expression in cell cultures and *Acs16* deficient animals. In addition, a comparison of *Glut4* mRNA between GM and OM was not performed in this study. Further investigation of this protein in membrane fractions and analysis of functional markers of glucose utilization, including glycogen synthesis and glucose oxidation rate, under long-term glucose treatment may provide a better understanding of the role of *Acs16* in glucose utilization in skeletal muscle.

GM has a high abundance of protein kinase C theta (PKC- θ), which interferes with insulin signaling [10], and the percentage composition of glycolytic fibers in skeletal muscle is positively correlated with the level of fasting plasma glucose [6]. However, a previous study utilizing whole skeletal muscle reported no significant changes in IRS-1 and Akt phosphorylation. Therefore, we investigated mTORc-1, FoxO-1, and p70S6K, which are the downstream effectors of IRS-1 and Akt. In this study, the phosphorylation of FoxO-1 and mTORc-1 and their downstream targets, p70S6K [26], was significantly enhanced in GM, while no change or slight increase in p70S6K was found in OM. *Acs16* deficiency in GM increased the phosphorylation of FoxO-1 and mTORc-1, but did not alter p70S6K. With higher TAG accumulation, no significant changes in these signaling molecules were detected in the OM of *Acs16* deficient mice. These findings are similar to those of a previous study on skeletal muscle-specific overexpression of *Dgat2*, suggesting that excessive lipid accumulation, specifically in OM, dissociates from insulin resistance in GM or whole muscle tissues [15]. Based on the data of this study, GM is a muscle fiber reactive to glucose supplementation,

although only FoxO-1 and mTORc-1 responded to glucose or *Acs16* suppression. Many studies have suggested that mTORc-1 and FoxO-1 interact with each other in cellular responses to nutrient availability [27,28]. FoxOs are important regulators that modulate the activity of Akt and mTORc-1 [27]. Akt-phosphorylated FoxO1 dissociates the TSC1/TSC2 complex, which activates mTORc-1, increases protein and lipid synthesis, and induces insulin resistance. Foxo-1 has been reported to be highly expressed in GM and parallel to the anti-fatigue ability of the GM muscle [29,30]. mTORc-1 activates p70S6K via inhibitory IRS-1-phosphorylation and elicits negative feedback to inhibit Akt [28]. Another study showed that mTORc-1 is sensitive to insulin action and substrate cycling owing to lipid accumulation [31]. Hence, FoxO-1 and mTORc-1 responded more sensitively to insulin than p70S6K, and glucose-induced insulin signaling was partially maintained in the GM. In contrast, mTORc-1 and its regulators have been reported to mediate immobilization-induced anabolic resistance in the soleus muscle [32], where a high proportion of OM exists. Due to the commitment of OM in long-term and continuous energy supply relative to GM [9], in OM, where FoxO-1 and mTORc-1 were not altered, the glucose-stimulated TAG increased to a similar extent as seen in GM in this study. Taken together, the difference in FoxO-1 and mTORc-1 phosphorylation and downstream insulin signaling between OM and GM is a novel finding of this study compared to previous studies that presented the signaling difference between GM and OM by mostly focusing on Akt, IRS and phosphatidylinositol 3 kinase (PI3K) signaling [33,34]. The findings of this study seem to be mediated by the enhanced insulin sensitivity of GM [27,28] and the properties of OM in long-term energy supply [9]. However, the results of this study have shown similar disparities in the activation of molecules in the insulin signaling cascade, as shown in previous studies: disassociation between insulin signaling and *Glut4* protein translocation within one type of skeletal muscle fiber [34], and inconsistencies in the phosphorylation of IRS and PI3K in both the soleus and extensor digitorum longus muscles [33]. Hence, the different responses in FoxO-1 and mTORc-1 phosphorylation between OM and GM in this study may not be conclusive, and a feed-forward mechanism among insulin signaling molecules in GM and OM needs to be addressed in future studies.

Overall, our data from previous studies [16,17] and current studies show that acyl-CoAs are unavailable for TAG synthesis in skeletal muscle if they have not been synthesized by *Acs16*. This study further showed that the inability of skeletal muscle fibers to synthesize TAG made *Acs16* deficient mice vulnerable to impaired insulin signaling. The discrepancy between decreased TAG and *Glut4* expression, but partially enhanced insulin signaling, can be explained by the dependence of *Acs16* deficient cells or muscle fibers on intracellular fatty acids limiting glucose uptake in skeletal muscle tissues. The metabolic profile observed was consistent with “athletes’ paradox” [4,12]; failure of muscle to use FA for TAG synthesis caused the *Acs16* deficient cells and mice to have improper insulin signaling and decreased glucose utilization. Such metabolic consequences due to *Acs16* suppression are somewhat different from the deficiency of *Acs11*, another main *Acs1* isoform in skeletal muscle. *Acs11*^{M/-} animals exhibit the inability of skeletal muscle to oxidize FA and vulnerability to systemic hypoglycemia [3,35]. Although the diabetic phenotype is relatively clear in *Acs11*^{M/-} mice, the phenotypic characteristics of *Acs16* knockdown in cells or animal models, in the context of insulin signaling responses and glucose utilization, have not been conclusive. Moreover, *Acs16* has a narrower substrate specificity and lower Km value for fatty acids than *Acs11* or *Acs14* [36], and may have limitations in protecting cells from the toxicity of lipids, including ceramides and phospholipid metabolites. Additionally, *Acs11* activity has been implicated in brown adipocyte energetics, and increased muscle TAG levels are associated with increased insulin sensitivity in *Acs11*^{M/-} mice [3,35]. Based on currently available reports, *Acs16* plays a role in

protecting cells from lipid-mediated toxicity rather than in the disturbance of lipid-mediated energy production or insulin signaling. As reported in neuronal cells, intensive profiling of lipid metabolites, including phospholipid species under complete *Acs16* deficient condition, may provide more insight into the role of *Acs16* in skeletal muscle.

In summary, the results from C2C12 cells under glucose supplementation were similar to those of our previous study [16], which revealed that *Acs16* suppression decreased basal glucose and fatty acid uptake and lipid storage in differentiated C2C12 skeletal myotubes. However, animal studies have shown that TAG accumulation decreased specifically in the OM of *Acs16* deficient animals while insulin signaling was enhanced only in the GM in this tissue. This result is different from our previous study utilizing whole skeletal muscle, which may have mixed types of muscle fibers, and did not show significant insulin signaling [17]. In addition, the cellular effects of *Acs16* suppression on TAG synthesis and insulin signaling observed under basal conditions were verified under glucose supplementation. Although this was a pilot study, it is meaningful in the context of verifying the distinguished role of different types of muscle fibers in *Acs16*-mediated lipid accumulation and signaling response. While we used glucose treatment for a very short period (30 minutes) to substitute insulin treatment in this study, high glucose treatment for prolonged time points has been shown to reduce the glucose transporter and impair the glucose response to insulin [37]. Since this study assessed the responses of these muscles under acute glucose supplementation, the *Acs16* mediating effects in high glucose challenges for prolonged time points need to be addressed in future studies.

SUMMARY

In this study, we investigated the effects of siRNA-mediated *Acs16* suppression on lipid accumulation in C2C12 cell-derived skeletal myotubes, GM fibers, and OM fibers of the skeletal muscle tissue of C57BL/6J mice under acute glucose supplementation. These results demonstrate distinctive differences in the pattern of lipid accumulation, *Glut4* expression, and insulin signaling among GM fibers and OM fibers. Increased FoxO-1 and mTORc-1 downstream insulin signaling in response to acute glucose supplementation was observed only in GM, which is contrary to our previous study, wherein no change or decrease was observed during insulin signaling in the skeletal muscle with mixed fiber type. Although the effects of *Acs16* on insulin signaling are still inconclusive, the results of this study addressed the importance of considering muscle fiber types separately to investigate lipid metabolism and insulin responses.

ACKNOWLEDGEMENT

The authors sincerely thank A. Kim and J.Y Lee for their assistance with animal care and sample analysis.

REFERENCES

1. Randle PJ, Garland PB, Hales CN, Newsholme EA. The glucose fatty-acid cycle. Its role in insulin sensitivity and the metabolic disturbances of diabetes mellitus. *Lancet* 1963; 281(7285): 785-789.
[PUBMED](#) | [CROSSREF](#)

2. Chavez JA, Summers SA. Characterizing the effects of saturated fatty acids on insulin signaling and ceramide and diacylglycerol accumulation in 3T3-L1 adipocytes and C2C12 myotubes. *Arch Biochem Biophys* 2003; 419(2): 101-109.
[PUBMED](#) | [CROSSREF](#)
3. Li LO, Grevengoed TJ, Paul DS, Ilkayeva O, Koves TR, Pascual F, et al. Compartmentalized acyl-CoA metabolism in skeletal muscle regulates systemic glucose homeostasis. *Diabetes* 2015; 64(1): 23-35.
[PUBMED](#) | [CROSSREF](#)
4. Pan DA, Lillioja S, Kriketos AD, Milner MR, Baur LA, Bogardus C, et al. Skeletal muscle triglyceride levels are inversely related to insulin action. *Diabetes* 1997; 46(6): 983-988.
[PUBMED](#) | [CROSSREF](#)
5. Ellis BA, Poynten A, Lowy AJ, Furler SM, Chisholm DJ, Kraegen EW, et al. Long-chain acyl-CoA esters as indicators of lipid metabolism and insulin sensitivity in rat and human muscle. *Am J Physiol Endocrinol Metab* 2000; 279(3): E554-E560.
[PUBMED](#) | [CROSSREF](#)
6. Lillioja S, Young AA, Culter CL, Ivy JL, Abbott WG, Zawadzki JK, et al. Skeletal muscle capillary density and fiber type are possible determinants of *in vivo* insulin resistance in man. *J Clin Invest* 1987; 80(2): 415-424.
[PUBMED](#) | [CROSSREF](#)
7. Kriketos AD, Pan DA, Lillioja S, Cooney GJ, Baur LA, Milner MR, et al. Interrelationships between muscle morphology, insulin action, and adiposity. *Am J Physiol* 1996; 270(6 Pt 2): R1332-R1339.
[PUBMED](#)
8. Rocchi A, Milioto C, Parodi S, Armirotti A, Borgia D, Pellegrini M, et al. Glycolytic-to-oxidative fiber-type switch and mTOR signaling activation are early-onset features of SBMA muscle modified by high-fat diet. *Acta Neuropathol* 2016; 132(1): 127-144.
[PUBMED](#) | [CROSSREF](#)
9. Philippi M, Sillau AH. Oxidative capacity distribution in skeletal muscle fibers of the rat. *J Exp Biol* 1994; 189: 1-11.
[PUBMED](#)
10. Donnelly R, Reed MJ, Azhar S, Reaven GM. Expression of the major isoenzyme of protein kinase-C in skeletal muscle, nPKC theta, varies with muscle type and in response to fructose-induced insulin resistance. *Endocrinology* 1994; 135(6): 2369-2374.
[PUBMED](#) | [CROSSREF](#)
11. Mullen KL, Pritchard J, Ritchie I, Snook LA, Chabowski A, Bonen A, et al. Adiponectin resistance precedes the accumulation of skeletal muscle lipids and insulin resistance in high-fat-fed rats. *Am J Physiol Regul Integr Comp Physiol* 2009; 296(2): R243-R251.
[PUBMED](#) | [CROSSREF](#)
12. Goodpaster BH, He J, Watkins S, Kelley DE. Skeletal muscle lipid content and insulin resistance: evidence for a paradox in endurance-trained athletes. *J Clin Endocrinol Metab* 2001; 86(12): 5755-5761.
[PUBMED](#) | [CROSSREF](#)
13. Fruebis J, Tsao TS, Javorschi S, Ebbets-Reed D, Erickson MR, Yen FT, et al. Proteolytic cleavage product of 30-kDa adipocyte complement-related protein increases fatty acid oxidation in muscle and causes weight loss in mice. *Proc Natl Acad Sci U S A* 2001; 98(4): 2005-2010.
[PUBMED](#) | [CROSSREF](#)
14. Dyck DJ, Peters SJ, Glatz J, Gorski J, Keizer H, Kiens B, et al. Functional differences in lipid metabolism in resting skeletal muscle of various fiber types. *Am J Physiol* 1997; 272(3 Pt 1): E340-E351.
[PUBMED](#)
15. Levin MC, Monetti M, Watt MJ, Sajan MP, Stevens RD, Bain JR, et al. Increased lipid accumulation and insulin resistance in transgenic mice expressing DGAT2 in glycolytic (type II) muscle. *Am J Physiol Endocrinol Metab* 2007; 293(6): E1772-E1781.
[PUBMED](#) | [CROSSREF](#)
16. Jung YH, Bu SY. Suppression of long chain acyl-CoA synthetase blocks intracellular fatty acid flux and glucose uptake in skeletal myotubes. *Biochim Biophys Acta Mol Cell Biol Lipids* 2020; 1865(7): 158678.
[PUBMED](#) | [CROSSREF](#)
17. Lee JY, Kim A, Jung YH. Dissociation of systemic glucose homeostasis from triacylglyceride accumulation by reduced *Acs16* expression in skeletal muscle. *Biotechnol Bioprocess Eng* 2018; 23(4): 465-472.
18. Bu SY, Mashek DG. Hepatic long-chain acyl-CoA synthetase 5 mediates fatty acid channeling between anabolic and catabolic pathways. *J Lipid Res* 2010; 51(11): 3270-3280.
[PUBMED](#) | [CROSSREF](#)
19. Mashek DG, Li LO, Coleman RA. Long-chain acyl-CoA synthetases and fatty acid channeling. *Future Lipidol* 2007; 2(4): 465-476.
[PUBMED](#) | [CROSSREF](#)

20. Bligh EG, Dyer WJ. A rapid method of total lipid extraction and purification. *Can J Biochem Physiol* 1959; 37(8): 911-917.
[PUBMED](#) | [CROSSREF](#)
21. Coleman RA. It takes a village: channeling fatty acid metabolism and triacylglycerol formation via protein interactomes. *J Lipid Res* 2019; 60(3): 490-497.
[PUBMED](#) | [CROSSREF](#)
22. Galante P, Mosthaf L, Kellerer M, Berti L, Tippmer S, Bossenmaier B, et al. Acute hyperglycemia provides an insulin-independent inducer for GLUT4 translocation in C2C12 myotubes and rat skeletal muscle. *Diabetes* 1995; 44(6): 646-651.
[PUBMED](#) | [CROSSREF](#)
23. Kahn CR, Crettaz M. Insulin receptors and the molecular mechanism of insulin action. *Diabetes Metab Rev* 1985; 1(1-2): 5-32.
[PUBMED](#) | [CROSSREF](#)
24. Zierath JR, Hawley JA. Skeletal muscle fiber type: influence on contractile and metabolic properties. *PLoS Biol* 2004; 2(10): e348.
[PUBMED](#) | [CROSSREF](#)
25. Armstrong RB, Phelps RO. Muscle fiber type composition of the rat hindlimb. *Am J Anat* 1984; 171(3): 259-272.
[PUBMED](#) | [CROSSREF](#)
26. Marabita M, Baraldo M, Solagna F, Ceelen JJ, Sartori R, Nolte H, et al. S6K1 is required for increasing skeletal muscle force during hypertrophy. *Cell Reports* 2016; 17(2): 501-513.
[PUBMED](#) | [CROSSREF](#)
27. Hay N. Interplay between FOXO, TOR, and Akt. *Biochim Biophys Acta* 2011; 1813(11): 1965-1970.
[PUBMED](#) | [CROSSREF](#)
28. Soliman GA, Acosta-Jaquez HA, Dunlop EA, Ekim B, Maj NE, Tee AR, et al. mTOR Ser-2481 autophosphorylation monitors mTORC-specific catalytic activity and clarifies rapamycin mechanism of action. *J Biol Chem* 2010; 285(11): 7866-7879.
[PUBMED](#) | [CROSSREF](#)
29. Kamei Y, Miura S, Suzuki M, Kai Y, Mizukami J, Taniguchi T, et al. Skeletal muscle FOXO1 (FKHR) transgenic mice have less skeletal muscle mass, down-regulated type I (slow twitch/red muscle) fiber genes, and impaired glycemic control. *J Biol Chem* 2004; 279(39): 41114-41123.
[PUBMED](#) | [CROSSREF](#)
30. Azad M, Khaledi N, Hedayati M. Effect of acute and chronic eccentric exercise on FOXO1 mRNA expression as fiber type transition factor in rat skeletal muscles. *Gene* 2016; 584(2): 180-184.
[PUBMED](#) | [CROSSREF](#)
31. Kleinert M, Sylow L, Fazakerley DJ, Krycer JR, Thomas KC, Oxbøll AJ, et al. Acute mTOR inhibition induces insulin resistance and alters substrate utilization *in vivo*. *Mol Metab* 2014; 3(6): 630-641.
[PUBMED](#) | [CROSSREF](#)
32. Shimkus KL, Jefferson LS, Gordon BS, Kimball SR. Repressors of mTORC1 act to blunt the anabolic response to feeding in the soleus muscle of a cast-immobilized mouse hindlimb. *Physiol Rep* 2018; 6(20): e13891.
[PUBMED](#) | [CROSSREF](#)
33. Song XM, Kawano Y, Krook A, Ryder JW, Efendic S, Roth RA, et al. Muscle fiber type-specific defects in insulin signal transduction to glucose transport in diabetic GK rats. *Diabetes* 1999; 48(3): 664-670.
[PUBMED](#) | [CROSSREF](#)
34. Krook A, Kawano Y, Song XM, Efendic S, Roth RA, Wallberg-Henriksson H, et al. Improved glucose tolerance restores insulin-stimulated Akt kinase activity and glucose transport in skeletal muscle from diabetic Goto-Kakizaki rats. *Diabetes* 1997; 46(12): 2110-2114.
[PUBMED](#) | [CROSSREF](#)
35. Li LO, Ellis JM, Paich HA, Wang S, Gong N, Altshuler G, et al. Liver-specific loss of long chain acyl-CoA synthetase-1 decreases triacylglycerol synthesis and beta-oxidation and alters phospholipid fatty acid composition. *J Biol Chem* 2009; 284(41): 27816-27826.
[PUBMED](#) | [CROSSREF](#)
36. Van Horn CG, Caviglia JM, Li LO, Wang S, Granger DA, Coleman RA. Characterization of recombinant long-chain rat acyl-CoA synthetase isoforms 3 and 6: identification of a novel variant of isoform 6. *Biochemistry* 2005; 44(5): 1635-1642.
[PUBMED](#) | [CROSSREF](#)
37. van Putten JP, Krans HM. Glucose as a regulator of insulin-sensitive hexose uptake in 3T3 adipocytes. *J Biol Chem* 1985; 260(13): 7996-8001.
[PUBMED](#) | [CROSSREF](#)